Hybrid Pu/Synthetic Talc/Organic Clay Ternary Nanocomposites: Thermal, Mechanical and Morphological Properties

Guilherme Dias[1], Manoela Prado[1], Rosane Ligabue[1,2], Mathilde Poirier[3], Christophe Le Roux[3], Pierre Micoud[3], François Martin[3] and Sandra Einloft[1,2]

[1]Programa de Pós-Graduação em Engenharia e Tecnologia de Materiais (PGETEMA) – Pontifícia Universidade Católica do Rio Grande do Sul (PUCRS). Porto Alegre, Brazil
[2]Faculdade de Química (FAQUI) – Pontifícia Universidade Católica do Rio Grande do Sul (PUCRS). Porto Alegre, Brazil
[3]ERT 1074 géomatériaux – GET UMR 5563 CNRS - Université de Toulouse – Toulouse, France

Received: 20 July 2017, Accepted: 13 October 2017

ABSTRACT

Polyurethane (PU) nanocomposites filled with inorganic particles, aiming at the improvement of mechanical and thermal properties, are well known. Unlike previous work we describe here the combination of two fillers, synthetic talc (silico-metallic mineral particles-SSMMP) with distinct hydrothermal processes (SSMMP 7 h and 24 h) and organically-modified commercial clay (SPR), aiming towards development of new polyurethane ternary nanocomposites by *in situ* polymerisation. Fillers were added 3 wt.% of the mass of pristine polymer, with a ranging of weight proportions (75:25/25:75) of SSMMP and SPR. Results were compared to those for nanocomposites containing pure SSMMP and SPR fillers. Dispersion degrees and filler interactions with the polyurethane matrix were followed by FTIR, XRD, SEM, TEM and AFM techniques. Results showed that the fillers presented a good dispersion and were exfoliated/well dispersed in the polyurethane matrix. Thermal and mechanical properties of nanocomposites were evaluated in comparison to the binary nanocomposites (PU/SSMMP 7 h, PU/SSMMP 24 h and PU/SPR). All nanocomposites presented superior values of Young's modulus to that of pristine PU. Results evidenced that the blend of SSMMP and SPR fillers is an interesting strategy to improve thermal and mechanical properties of nanocomposites.

Keywords: polyurethane; synthetic talc; ternary nanocomposites; organic clay; mechanical properties

1. INTRODUCTION

Polyurethanes are multifunctional polymers whose properties can be easily tailored by changing their molecular structures of 'soft segment' and 'hard segment'. To improve polyurethane properties, a common method is to add inorganic particles to the polymer matrix. The high aspect ratio of reinforcing particles such as talc, mica, silica, clay and calcium carbonate is of great importance to further increase polymers thermo-mechanical properties[1]. The best performance of polymeric nanocomposites is achieved when the silicate layers are well dispersed in the polymer matrix. Depending on the polymer's degree of interaction with the layered silicate mineral particles, hybrids nanocomposites are obtained with structures ranging from intercalated to exfoliated[2–4]. Talc, a layered magnesium silicate mineral with ideal formula $Mg_3Si_4O_{10}(OH)_2$ is used as filler in composite materials to reduce their production costs, improve their physical and chemical properties, and/or to offer new functionalities[5,6]. Montmorillonite (MMT) is also a layered silicate, but its structure consists of octahedral sheet of alumina sandwiched between two external silica tetrahedrons. The specificity of MMT is due to the presence in the interlayer of hydrated cations. MMT is a swellable clay mineral[7]. Polymer/clay nanocomposites have become important due to their improvements in mechanical strength and stiffness, thermal stability and

*Correspondent author:
E-mail: einloft@pucrs.br

gas barrier properties[8–10]. Layered silicates have often been described in the literature as fillers due to the availability of clay materials[11]. Natural talc ores consist in a mixture of several minerals, exhibiting some cationic substitutions[12] and consequently are inhomogeneous in chemical structure, crystalline phase and size distribution[13]. Manufacture of synthetic talc with a well-defined chemical composition and high purity, besides the possibility of the crystallinity, particle size and layer thickness control is a viable alternative. For example, by varying by a few tens of degrees the temperature of hydrothermal reaction, the average particle size can vary by several hundreds of nanometres[14,15]. The advantage of polymer nanocomposites is that the improvement in their properties can be achieved with a low percentage of layered silicates[16]. Several matrix polymers have been used to obtain polymer-layered silicate nanocomposites including polyurethane[1–5,7,8,10,16–34], PMMA[9], blends[14,35–40], polypropylene[41–43], polyamides[44], polylactide[45,46], polystyrene[47] and EVA[48]. In previous studies, our group investigated the performance of PU/synthetic talc nanocomposites with different filler percentages. Best results were obtained when a loading of 3 wt.% was used[21–23]. To further improve the performance of nanocomposites, the use of filler mixtures has been described. Alavi et al. produced ternary nanocomposites of PP/talc/nanoclay resulting in materials showing a better filler dispersion and an increase in mechanical properties[49]. Aguilar et al. prepared PP-based nanocomposites with organically modified montmorillonite (oMMT) and different types of $CaCO_3$ via melt blending. The resulting materials presented enhanced dispersion and better mechanical and thermal properties[50]. Kodal et al. investigated the mechanical, thermal and morphological properties of PA6 hybrid composites containing talc and wollastonite[51]. Garmabi et al. produced HDPE/nanoclay/nano $CaCO_3$ nanocomposites evidencing that the co-incorporation of this fillers improved nanocomposites' mechanical properties[52].

In this work, new polyurethane based nanocomposites were obtained by *in situ* polymerisation by mixing synthetic silico-metallic mineral particles produced by different hydrothermal treatments; SSMMP 24 h/205°C (SSMMP 24 h) and SSMMP 7 h/315°C (SSMMP 7 h) and SPR clay in different weight proportions (75:25 and 25:75) of fillers (3 wt.% regarding the mass of pristine polyurethane) were obtained.

2. EXPERIMENTAL

2.1 Materials

Polycaprolactone diol (PCL) MM: 2000 g/mol by Aldrich, hexamethylene diisocyanate (HDI) by Merck; dibutyltin dilaurate (DBTDL) by Miracema-Nuodex Ind. and methyl ethyl ketone (MEK) by Merck were used as received. Magnesium acetate tetrahydrate $(CH_3COO)_2Mg.4H_2O$), sodium metasilicate pentahydrate ($Na_2SiO_3.5H_2O$), sodium acetate trihydrate ($CH_3COONa.3H_2O$) and acetic acid were used for the syntheses of SSMMP powders (24 h/205°C and 7 h/ 315°C). All reagents were purchased from Aldrich and used without any further purification[6]. Samples were prepared as described elsewhere[53]. Organically modified commercial clay Rheotix SPR was donated by Nokxeller. Fillers were added in a percentage of 3 wt% relative to the pristine polymer without any treatments. Proportions of 75:25/25:75 of synthetic talc and SPR clay respectively, were used.

2.2 Hybrid Nanocomposites Obtained by *in situ* Polymerisation

The dispersion of SSMMP and SPR clay (in the desired proportions) was carried out in ultrasound bath (40 kHz) for 60 min, utilising methyl ethyl ketone as solvent. A glass reactor of 500 mL equipped with five inputs was used to perform the reactions. Mechanical stirring, thermocouple (to maintain the temperature at 40°C), reflux system and an addition funnel were connected to the reaction system. The reaction occurred in one step. Polycaprolactone diol (PCL) MM: 2000 g/mol, hexamethylene diisocyanate (HDI) (molar ratio between PCL and HDI = 1.1:1), DBTDL as catalyst (0.1% regarding the mass of reagents) and methyl ethyl ketone (MEK) as solvent (≅100 mL) as well as the fillers were added to the reactor. First, PCL was heated to melt with MEK. After that, a mixture of SSMMP/SPR (in the desired proportions) and the catalyst (DBTDL) were placed in the reactor. HDI was placed slowly, at the end of its addition the reaction started and was kept under reflux for 2 h and 30 min in an inert atmosphere (N_2). Lastly, films with ≅ 0.1 mm of thickness were produced by casting and dried at room temperature.

2.3 Testing and Characterisation

2.3.1 X-ray Diffraction (XRD)

Fillers in a form of powder and hybrid nanocomposites in the form of films were analysed by X-ray diffraction (XRD) recorded on a Shimadzu XRD-7000 diffractometer with CuKα Bragg-Brentano geometry θ-θ radiations, between 5 and 80 degrees with a step size of 0.02 degrees, current of 40 kV and voltage of 30 mA.

2.3.2 Transmission Electron Microscopy (TEM)

Transmission electron microscopy (TEM) was used to determine the morphology and dispersion

degree of hybrid nanocomposites. Samples of the hybrid nanocomposites in the form of films were cryomicrotomed and samples of the fillers were dispersed in water to obtain TEM images, utilising the equipment Tecnai G2 T20 FEI operating at 200 kV.

2.3.3 Fourier Transfer-infrared (FTIR) Spectroscopy

Fourier transform infrared spectroscopy (FTIR-Perkin Elmer FTIR spectrometer model Spectrum 100) was used to reveal the structural properties of fillers (powders) and hybrid nanocomposites (films), scanned from 650–4000 cm^{-1} utilising a UATR accessory.

2.3.4 Thermogravimetric Analysis (TGA)

Thermogravimetric analysis were performed to ascertain the thermal decomposition of pristine PU and hybrid nanocomposites in a SDT equipment (TA Instruments Model Q600), tests were carried out in a temperature range from 25°C to 800°C with a heating rate of 20°C min^{-1} under constant N_2 flow, utilising pristine PU and hybrid nanocomposites films and performed in triplicate.

2.3.5 Differential Scanning Calorimetry (DSC)

Melting temperature (Tm) and crystallisation temperature (Tc) of pristine PU and hybrid nanocomposites films were obtained by Differential Scanning Calorimetry (DSC) (TA Instruments model Q20 equipment). The tests were carried out under N_2 in a temperature range from −90°C to 200°C with a heating/cooling rate of 10°C min^{-1}, in two heating cycles.

2.3.6 Dynamic Mechanical Analysis (DMA)

Tensile tests (stress/strain) of pristine PU and hybrid nanocomposites were performed in DMTA equipment (TA Instruments Model Q800); tests were carried out at 25°C with rectangular shape films (thickness ~0.10 mm, length 12 mm, width ~7.0 mm) at 1 N min^{-1}. ASTMD638 was used to determine the Young moduli of samples. Analyses were carried out in triplicate until the rupture of samples.

2.3.7 Field Emission Scanning Electron Microscopy (FESEM)

Field emission scanning electron microscopy (FESEM) analyses were performed in FEI Inspect F50 equipment in secondary electrons (SE) mode and used for assessment of filler distributions in the polymer matrix. The samples (films) were placed in a stub and covered with a thin gold layer.

2.3.8 Atomic Force Microscopy (AFM)

Atomic force microscopy (AFM) was used to collect roughness data of pristine PU and hybrid nanocomposites. The cryomicrotomed samples were used to obtain the data. Analyses were performed in tapping mode to construct phase/height contrast images at different locations on the top surface of the samples using a Bruker Dimension Icon PT equipped with a TAP150A probe (Bruker, resonance frequency of 150 kHz and 5 N m^{-1} spring constant). The equipment was calibrated prior sample measurements. Scanned area of the images was 5 × 5 μm^2 with a resolution of 512 frames per area.

3. RESULTS AND DISCUSSIONS

3.1 X-ray Diffraction Analysis (XRD)

Crystalline structure of fillers (SSMMP 7 h and SPR clay) and hybrid nanocomposites were evaluated by XRD (**Figure 1**). The XRD pattern for SSMMP 7 h (**Figure 1g**) presents low intensity enlarged peaks meaning synthetic talc are formed by coherent domains with a small number of layers[14,22,23]; evidencing that crystal sizes of synthetic talc are smaller than those of natural talc which present well-defined and intense peaks in the XRD spectrum[6,22,23].

The diffractograms of fillers and hybrid nanocomposites indicated that the peak associated with the fillers ($2\theta \cong 20°$) disappeared in the nanocomposites diffractograms, indicating a good dispersion of the fillers and suggesting that silicate layers are exfoliated within the polymeric chains[33]. Baniasadi et al. described the same behaviour for PP/clay nanocomposites synthesised by *in situ* polymerisation[41]. Garmabi et al. noticed that for HDPE/nanoclay/nano $CaCO_3$, the intensity of ternary nanocomposites X-ray peaks were reduced, indicating intercalated/exfoliated morphology[52]. Likewise the diffraction peak associated with the polyurethane crystalline phase decreases for the hybrid nanocomposites indicating that the filler is well dispersed into the polymer matrix due to the interaction filler–polymeric chain[24,25]. It can be highlighted that even with two fillers mixed into the polyurethane matrix, a good dispersion was obtained, presumably due to the fillers hydroxyl groups interacting with the polyurethane chains[21,24,25].

3.2 Transmission Electron Microscopy (TEM)

From TEM images (**Figure 2** and **Figure 3**), it can be seen that for all systems individual particles and some local aggregates are present. TEM images also demonstrated that the combination of fillers did not

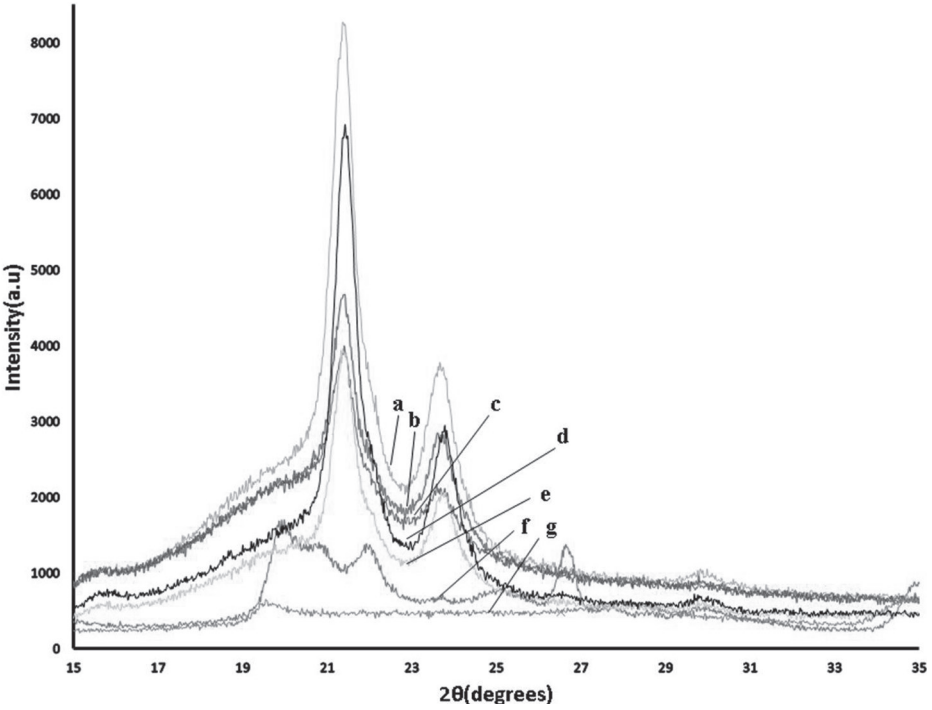

Figure 1. X-ray diffractogram patterns (a) PU, (b) PU/SSMMP 7 h+SPR 3% 25:75, (c) PU/SSMMP 7 h+SPR 3% 75:25, (d) PU/SPR 3%, (e) PU/SSMMP 7 h 3%, (f) SPR clay and (g) SSMMP 7 h

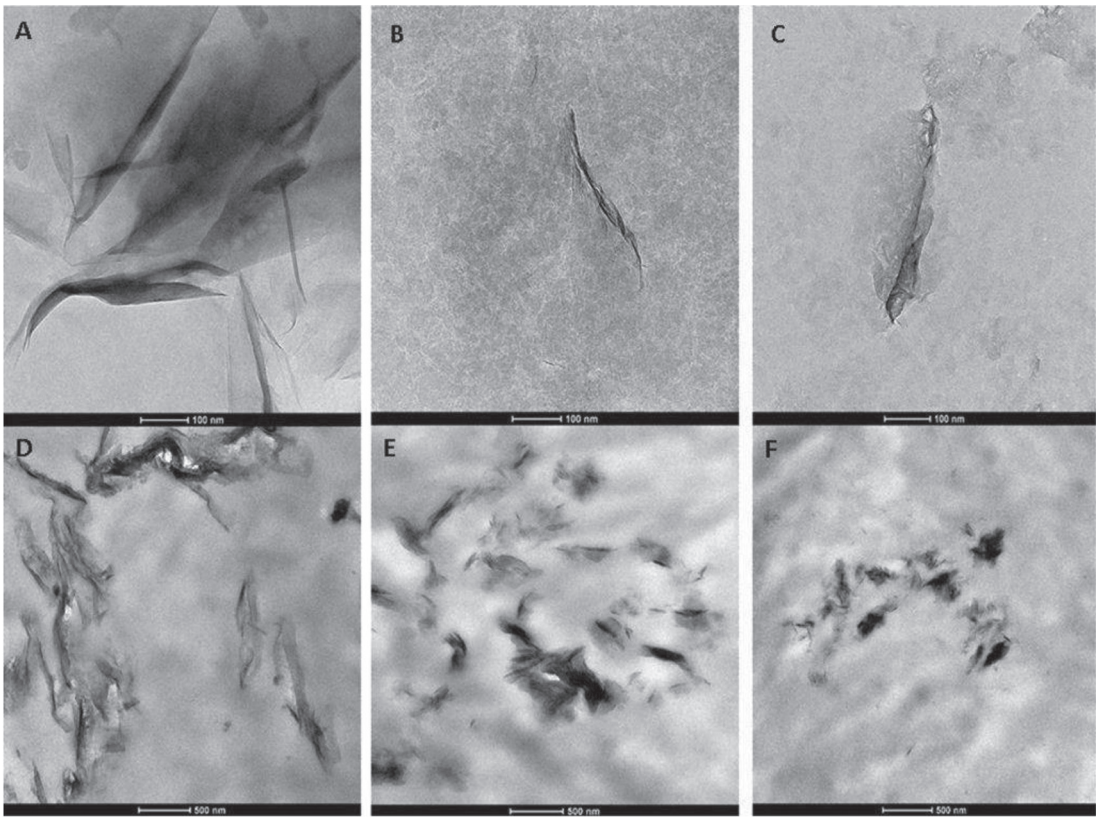

Figure 2. TEM micrographs of (a) SPR clay, (b) SSMMP 7 h, (c) SSMMP 24 h, (d) PU/SPR 3%, (e) PU/SSMMP 7 h 3% and (f) PU/SSMMP 24 h 3%

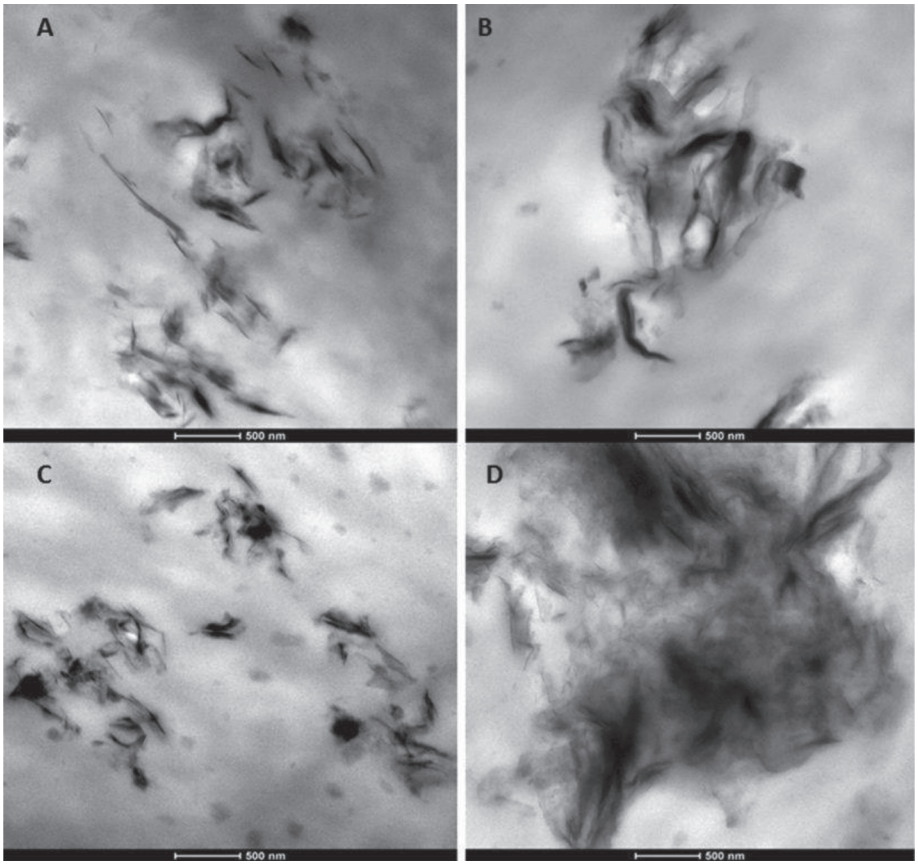

Figure 3. TEM micrographs of (a) PU/SSMMP7h+SPR 3% 75:25, (b) PU/SSMMP 7 h+SPR 3% 25:75, (c) PU/SSMMP 24 h+SPR 3% 75:25 and (d) PU/SSMMP 24 h+SPR 3% 25:75

negatively affect their good dispersion. Dark entities indicate the cross-section of intercalated or stacked clay layers; these stacked silicate layers are due to agglomeration. The bright fields in TEM micrograph represent the matrix[4,45,48].

As seen in TEM micrographs (**Figure 2** D-F and **Figure 3**), some intercalated structures can be seen along with exfoliated ones. Yet, XRD results indicated the presence of exfoliated morphology, probably related to the fact that the total number of intercalated structures, was too insignificant to provide a prominent peak in XRD diffractogram[10]. **Figure 2** and **Figure 3** prove that the layers are arranged parallel and well dispersed in the polyurethane matrix probably reflecting in the thermal and mechanical properties[7].

3.3 Fourier Transform Infrared Spectroscopy (FTIR)

FTIR was performed to evaluate the structure of hybrid nanocomposites, the fillers (SSMMPs and SPR clay) and the neat PU, as seen in **Figure 4-I**. Bands assignments of SSMMPs and SPR clay were fulfilled regarding the characteristic vibrational modes described in literature. In the spectrum of SPR clay (**Figure 4-Ig**), it can be seen that clay particles produced characteristic bands associated with stretching vibration of Si—O in Si—O—Si groups of tetrahedral sheet around 1000 cm^{-1} and small bands at 915 and 800 cm^{-1} assigned to Si—O stretching and Al—Al—OH and Al—Mg—OH (present on the edges of the clay platelets) hydroxyl bending vibrations. The absorption band at 3626 cm^{-1} is assigned to stretching vibrations of Al—OH and the hydrogen-bonded water bending band at 1633 cm^{-1}. Bands at 2930 and 2858 cm^{-1} were due to the asymmetric and symmetric –CH stretching vibrations related to the alkylammonium group, at 1460 cm^{-1} for C-H bending, and around 753 cm^{-1} the symmetric Si—O—Si stretching mode is observed[4,19,54].

In the spectrum of neat SSMMP 7 h (**Figure 4-If**), the Mg_3OH band appears at 3679 cm^{-1} and the bands around 3400 cm^{-1} and 1629 cm^{-1} are related to

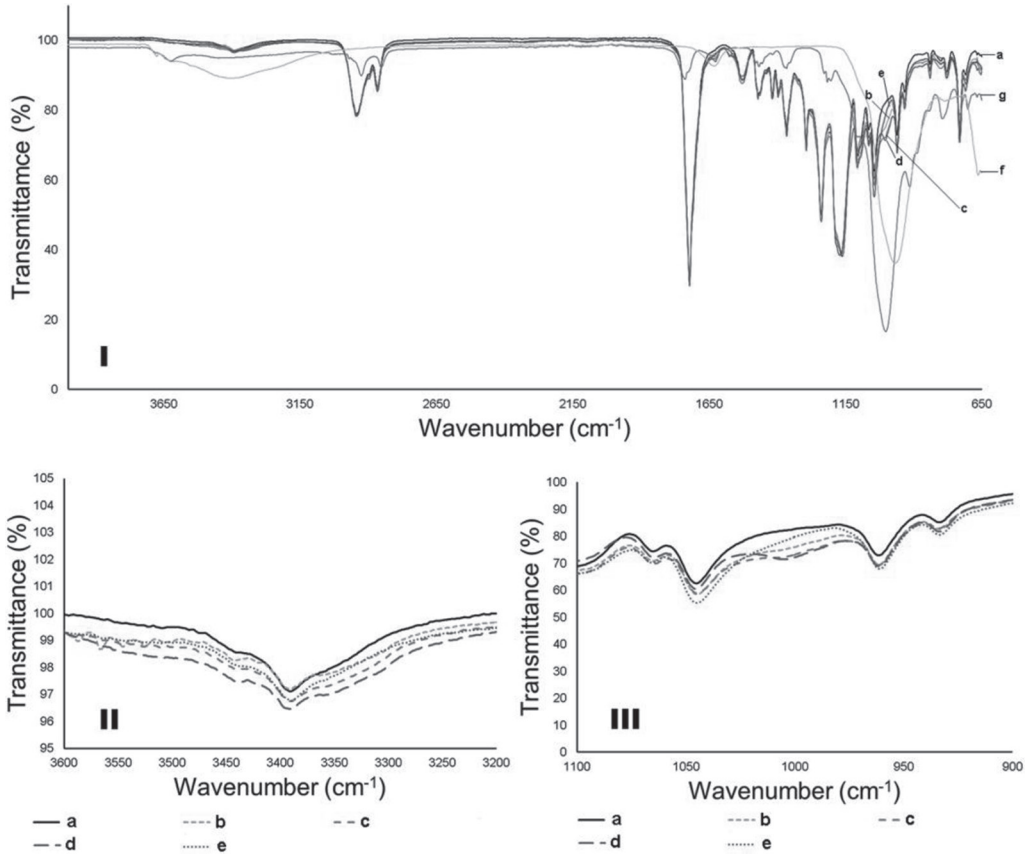

Figure 4. FTIR spectra of (a) PU pure, (b) PU/SSMMP 7 h+SPR 3% 25:75, (c) PU/SSMMP 7 h+SPR 3% 75:25, (d) PU/SSMMP 7 h 3%, (e) PU/SPR 3%, (f) SSMMP 7 h and (g) SPR clay in different wavenumber I (4000–650 cm^{-1}), II (3600–3200 cm^{-1}) and III (1100–900 cm^{-1})

the (Mg_2) O—H stretching[12]. At 1000 and 990 cm^{-1}, stretching vibrations of Si—O—Si appeared[12,22,23,55,56]. For neat PU, hybrid nanocomposites PU/SSMMP 7 h+SPR 75:25 3%, PU/SSMMP 7 h+SPR 25:75 3% and the nanocomposites PU/SSMMP 7 h 3% and PU/SPR 3% (**Figure 4-Ia-e**), the band at 3396 cm^{-1} corresponds to the urethane bonds (NH). Bands at 2946 and 2862 cm^{-1} are related to CH_2 vibrational modes. The C═O band of the urethane bonds appears at 1725 cm^{-1}. Bands around 1536 cm^{-1} represent the CN and NH bonds of the urethane groups. CO—O group bands at 1243 and 1172 cm^{-1}, and the band at 730 cm^{-1} corresponds to other vibrational modes of the CH_2 group[20–25,33]. In **Figure 4-II**, the augmentation of the band around 3400 cm^{-1} for the nanocomposites indicates that available hydroxyl groups of fillers are interacting with N-H urethane bonds of the polyurethane chains[20–25]. In **Figure 4-III**, the FTIR spectra of the nanocomposites present a new band near 1000 cm^{-1}, that can be associated with Si—O and Si—O—Si bonds stretching vibrational modes of the fillers, attesting that the fillers are incorporated into the polyurethane matrix, as noticed by our group in previous studies[22–25].

3.4 Thermogravimetric Analysis (TGA)

An increase on onset temperatures of hybrid nanocomposites with filler addition (**Figure 5**) was evidenced. Neat PU presented the lowest degradation temperature (302°C). The presence of blended fillers improved thermal stability of the hybrids (PU/SSMMP 7 h+SPR clay ≅ 336°C and PU/SSMMP 24 h+SPR clay ≅ 337°C). It can be highlight that the nanocomposites with SSMMPs presented higher values of degradation temperature[22,23] compared to the nanocomposite with SPR clay (PU/SSMMP 7 h, 340°C; PU/SSMMP 24 h, 337°C and PU/SPR, 326°C). This behaviour can be associated with filler dispersion into the polyurethane matrix. PU/SSMMP nanocomposites are better exfoliated[22,23] than PU/SPR nanocomposite, corroborating with TEM discussions. Also, SSMMPs even at lower concentrations appears to be more important when thermal properties are evidenced.

Observing DTG curves (%/°C) (**Figure 6**), an augmentation of the second peak is noticed in samples with SSMMP and SSMMP+SPR clay. In the SPR clay

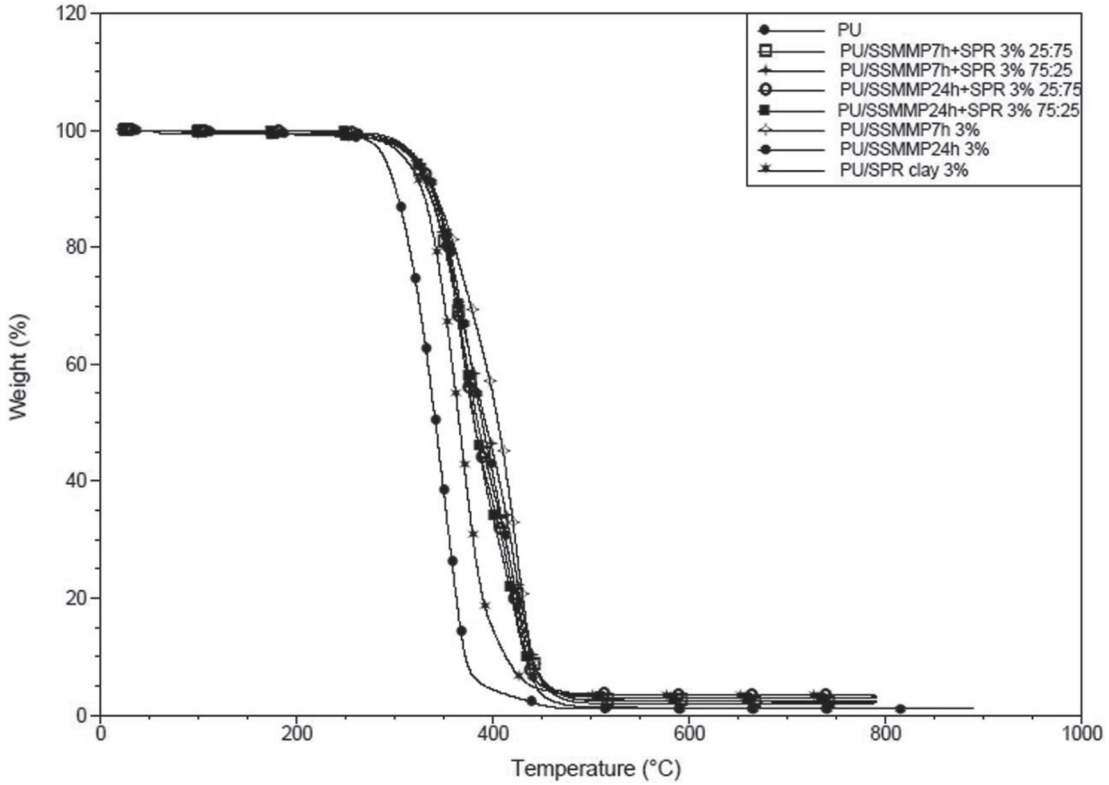

Figure 5. TGA curves for the pristine PU and the hybrid nanocomposites

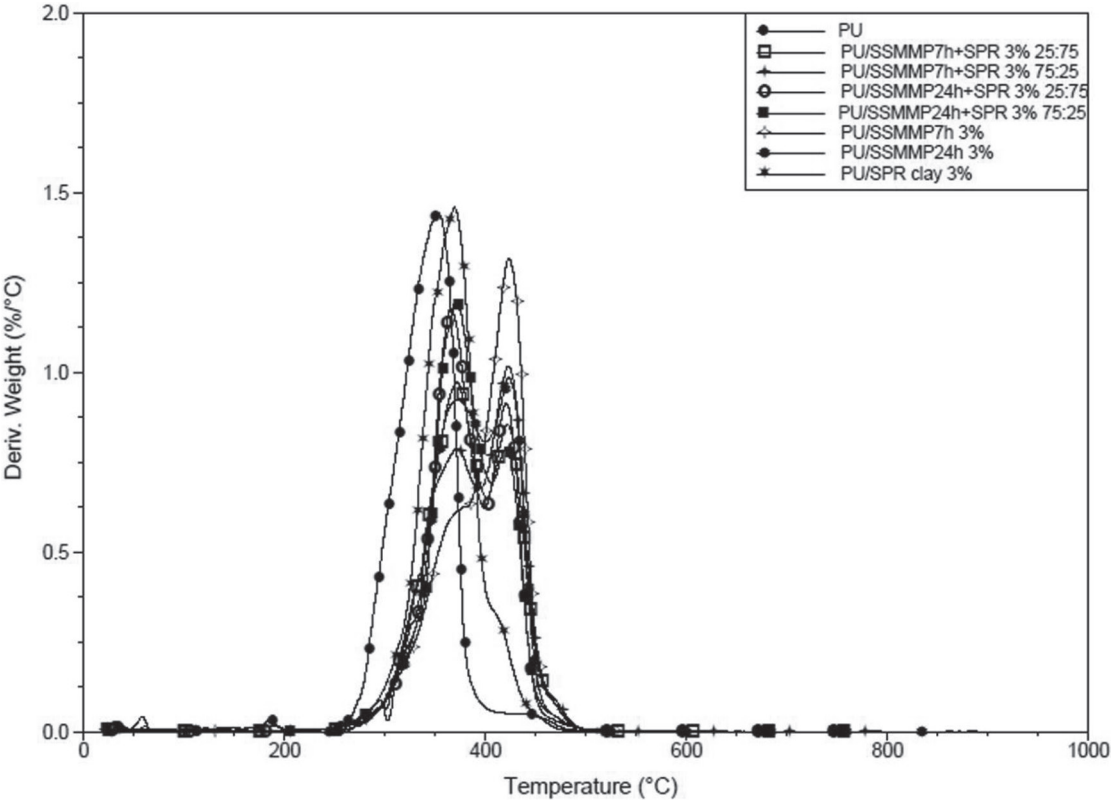

Figure 6. DTGA curves (%/°C) versus temperature of the pristine PU and the hybrid nanocomposites

Table 1. Results obtained by DSC analysis for the nanocomposites

Samples	Tc (°C)	Tm (°C)	△Hc (J/g)	ΔHm (J/g)
PU	0.26	37.61	33.40	33.49
PU/SSMMP7 h+SPR 3% 75:25	1.49	37.34	30.91	31.52
PU/SSMMP7 h+SPR 3% 25:75	−0.56	37.34	28.25	29.32
PU/SSMMP24 h+SPR 3% 75:25	0.33	37.77	33.80	35.34
PU/SSMMP24 h+SPR 3% 25:75	−1.53	37.45	28.60	32.11
PU/SSMMP7 h 3%	6.31	40.24	39.85	39.40
PU/SSMMP24 h 3%	5.95	40.10	40.75	41.92
PU/SPR 3%	8.29	44.79	41.12	42.96

sample, this behaviour was not observed. The hydroxyl groups of SSMMP can form a network structure with polyurethane chains as described in literature[22,23,44] and be responsible for the appearing of the second peak on DTG curves (**Figure 6**).

As described elsewhere thermal stability of pristine PU is improved by the presence of clay-layered crystals, which form a maze or 'tortuous path' in the PU matrix[10]. The incorporation of clay into the polymer matrix enhanced thermal stability by acting as a superior insulator and mass transport barrier to volatile products. These results can be attributed to dispersion and barrier effects of the clay layers against oxygen diffusion through the matrix[26,31,32,41,45].

3.5 Differential Scanning Calorimetry (DSC)

Table 1 presents the crystallisation temperatures (Tc) of hybrid nanocomposites. Tc temperatures of hybrid nanocomposites slightly changed once compared to neat PU, suggesting that the nucleating effect of the combined fillers is less important than when they are not blended. When fillers are combined the exfoliated structures restrict the movement of the polymeric chains retarding the crystallisation of the matrix[57]. For samples obtained with SSMMP (7 h and 24 h) and SPR clay an increase in the crystallisation temperatures values were observed. This behaviour is well known when talc and clay are added as fillers, and it is frequently reported that plate-like fillers are good nucleating agents because of their high aspect ratios[22,24,41,42,45]. For melting temperatures values the same behaviour was observed.

3.6 Dynamic Mechanical Analysis (DMA)

Stress–strain results are seen in **Figure 7**. All hybrid nanocomposites with SSMMP 7 h/24 h/SPR clay samples presented greater values of stress to small deformations when compared to PU. Fillers addition made the materials more rigid, most likely because the fillers (SSMMPs and SPR clay) and the polyurethane matrix formed crosslinks resulting from hydrogen bonding, as seen in FTIR[20–25].

Figure 8 exhibits the Young's modulus for neat polyurethane and hybrid nanocomposites. Young's modulus values presented a significant augmentation, suggesting that the materials stiffness at lower stress was affected as usual by fillers incorporation. The nanocomposite filled with SPR clay presented the higher value (366 MPa). The nanocomposite filled with SSMMP 7 h+SPR clay 25:75 presented a larger value for Young's modulus of 238 MPa, while the pristine PU presented 92 MPa (**Figure 8**). SSMMPs seem to influence directly mechanical behaviour of hybrids. But Young's Modulus augmentation is more pronounced when SPR clay is added. Young's modulus augmentation is attributed to the reinforcement provided by the dispersed fillers with a large aspect ratio, which reduces the molecular mobility of polymer chains, consequently stiffening the material[22,33]. Garmabi et al. described that for HDPE/nanoclay/nano $CaCO_3$ systems the reinforcing effect of the nanoclay was superior to $CaCO_3$, due to the nanoclay's large aspect ratio[52].

Therefore, the increase in the Young's modulus can be associated with the interfacial interaction between silicate layers and polyurethane matrix[17,29,43,45]. The surface area and shape play an important role in these properties. Yousfi et al. also related a significant increase of 39.4% on the Young's Modulus in PP/PA6 blends filled with synthetic talc (1880 MPa for the PP/PA6 blends and 2620 MPa with synthetic talc)[14] and our group noticed a maximum increment to the sample PU/synthetic Ni-talc 1 wt%, which presented an increase of 5.7% when compared to pristine PU, and an increase

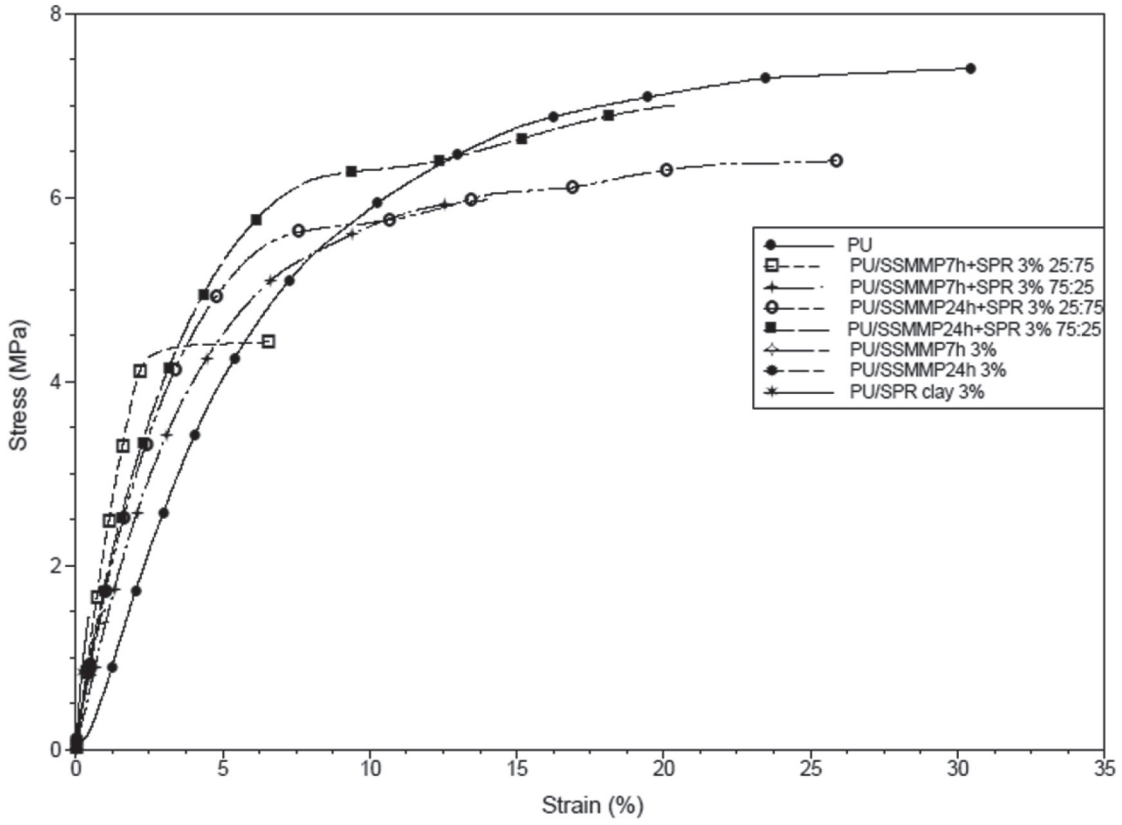

Figure 7. Stress x Strain, by DMA, for the hybrid nanocomposites and pristine PU

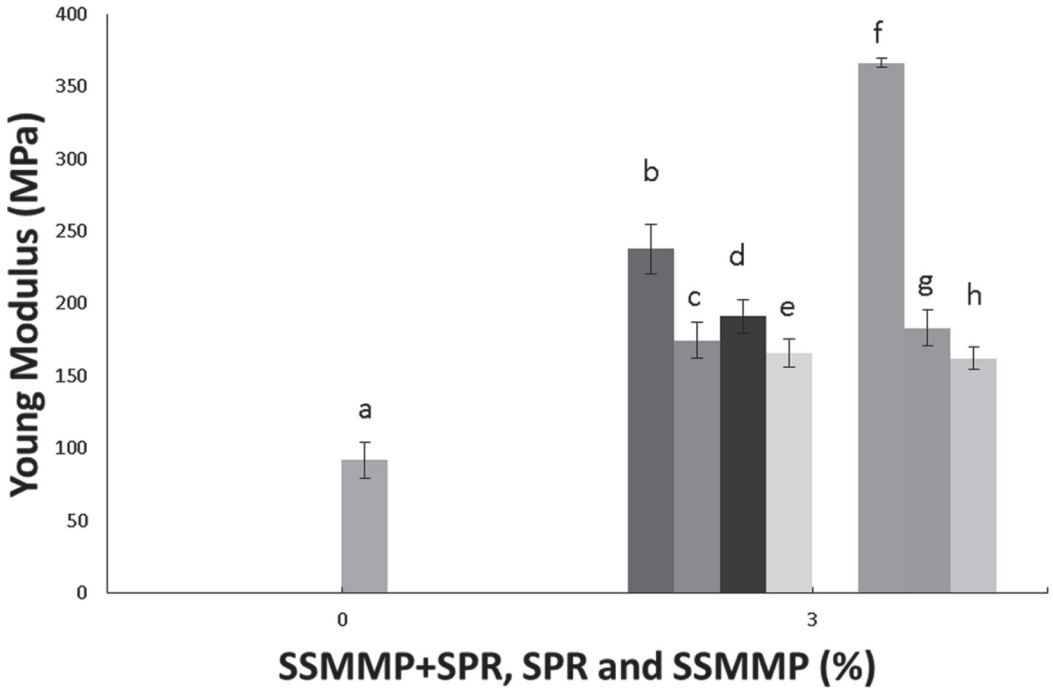

Figure 8. Young's modulus values for hybrid nanocomposites and pristine PU (a) PU Pure; (b) PU SSMMP 7 h+SPR 3% 25:75; (c) PU SSMMP 7 h+SPR 3% 75:25; (d) PU SSMMP 24 h+SPR 3% 25:75, (e) PUSSMMP 24 h+SPR 3% 75:25, (f) PU/SPR clay 3%, (g) PU/SSMMP 7 h 3% and PU/SSMMP 24 h 3%

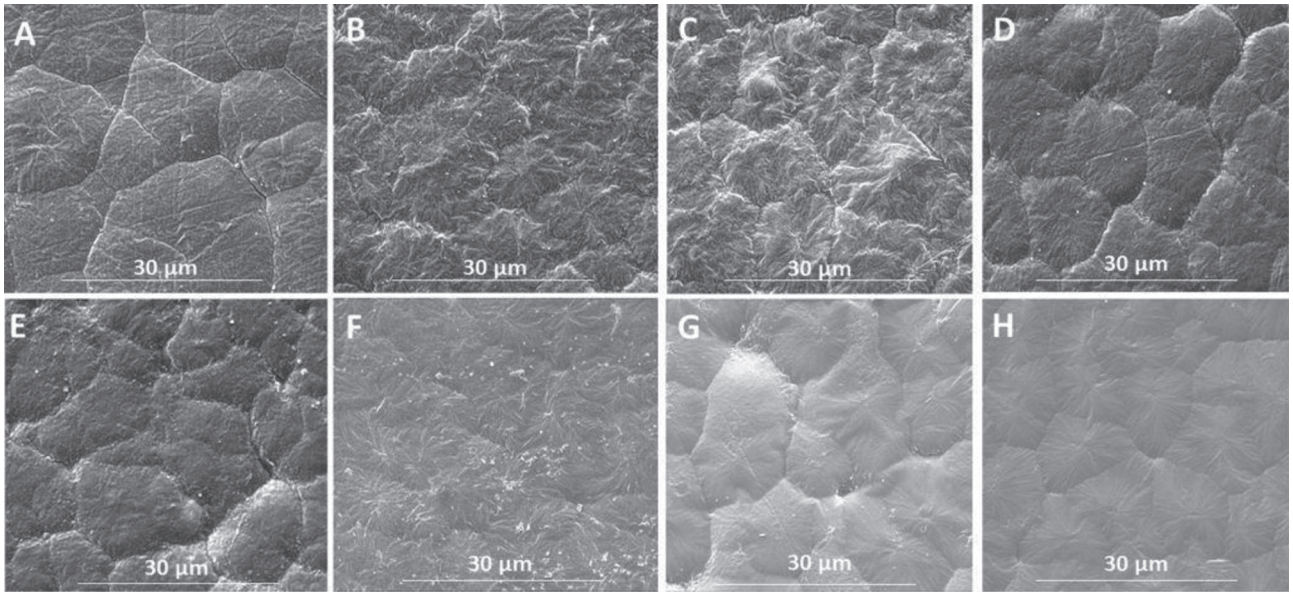

Figure 9. Micrographs, mode SE, of the materials at magnification of 5000x. (a) PU pure, (b) PU/SSMMP 7 h+SPR 3% 75:25, (c) PU/SSMMP 7 h+SPR 3% 25:75, (d) PU/SSMMP 24 h+SPR 3% 75:25, (e) PU/SSMMP 24 h+SPR 3% 25:75, (f) PU/SSMMP 7 h 3%, (g) PU/SSMMP 24 h 3% and (h) PU/SPR 3%

of 65% on the sample PU/SSMMP 7 h 3 wt%[21,22]. Therefore, when both fillers are placed together into the polyurethane matrix it is possible to obtain hybrid nanocomposites with superior mechanical properties.

3.7 Field Emission Scanning Electron Microscopy (FESEM)

On the basis of the morphological study of the prepared hybrid materials, as seen in **Figure 9**, it can be noticed that the achieved dispersion of the fillers into the polyurethane matrix was uniform and homogeneous[37]. Defects and stress concentration sites are prevented without the formation of agglomerated particles[22,35]. Good filler dispersion generated a superior contact area between matrix/filler, switching molecular mobility and consequently thermo-mechanical properties of the matrix[22,29]. **Figure 9** evidences that nucleation sites were formed in all hybrid nanocomposites; these morphological changes associated with a good dispersion of fillers and fillers-polymer interaction are probably promoting the different thermo-mechanical properties of hybrid nanocomposites[22,24].

Figure 10 shows SEM images of cryogenically fractured surface of pristine PU and hybrid nanocomposites. For pristine PU (**Figure 10A**), the appearance of grooves occurred randomly distributed on the cryo-fractured surface which looks more flat and smoother, presenting no important voids[22,23]. A different behaviour can be seen for the hybrid nanocomposites' cryo-fractured surfaces (**Figure 10B-H**). Hybrid nanocomposites presented a rough cryo-fractured surface full of voids and cracks. Similar results were found for PU/synthetic talcs, PLA/talc, PLA/clay and PLA blends composites[23,38,39,46]. An increase in the clay content modified the fracture profile, with an increase of the surface roughness, corroborating with mechanical properties results.

3.8 Atomic Force Microscopy (AFM)

A 3D height image of pristine PU and hybrid nanocomposites is shown in **Figure 11**. The hard segments appear bright due to their higher hardness, which resist penetration by the AFM probe tip. The soft segments appear with a darker contrast as they can be penetrated relatively easily by the AFM probe tip[10]. Addition of SSMMPs and SPR clay affected the morphology of this hard-soft segmental arrangement, especially when the interactions were on the nanoscale. With the addition of fillers, average roughness (Ra), root mean square roughness (Rq) and maximum height roughness (Rmax) had increased (**Table 2**). The higher values of these parameters comparing to pristine PU confirms the presence of filler particles on the surface, as reported in literature[31]. It can be seen from **Figure 11** that the layers of the fillers are well distributed both in soft and hard domain of the matrix. The presence of hydroxyl groups in both fillers seemed to significantly

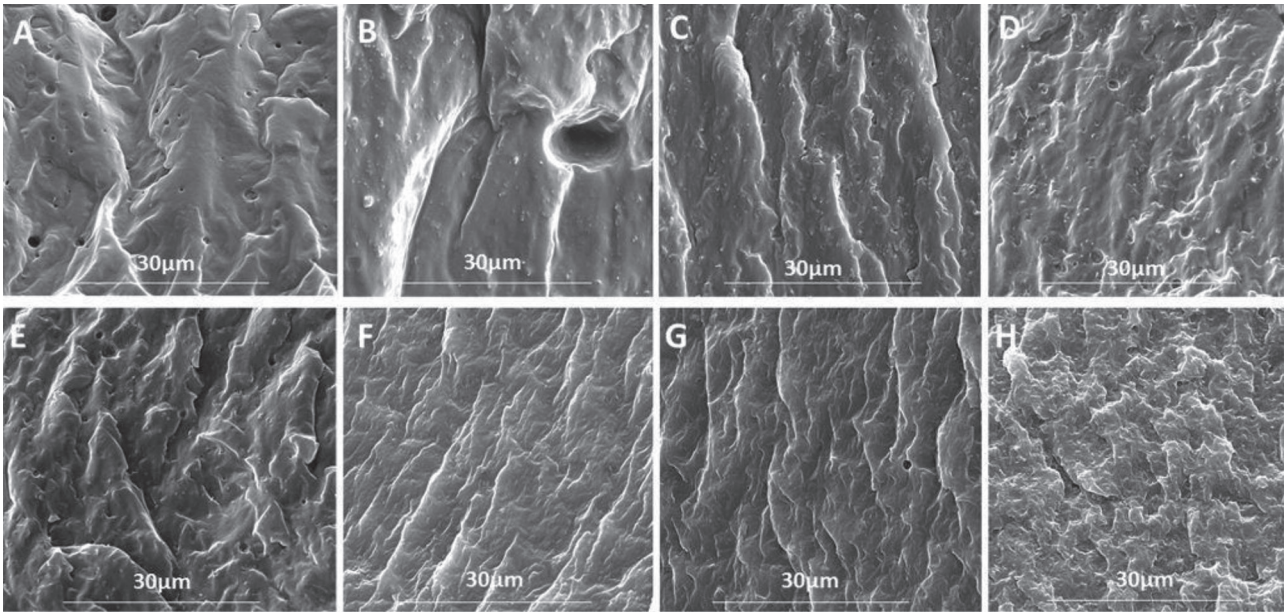

Figure 10. Micrographs from fractures, mode SE, of the materials at magnification of 5000x. (a) PU Pure, (b) PU/SSMMP 7 h+SPR 3% 75:25, (c) PU/SSMMP 7 h+SPR 3% 25:75, (d) PU/SSMMP 24 h+SPR 3% 75:25, (e) PU/SSMMP 24 h+SPR 3% 25:75, (f) PU/SSMMP 7 h 3%, (g) PU/SSMMP 24 h 3% and (h) PU/SPR 3%

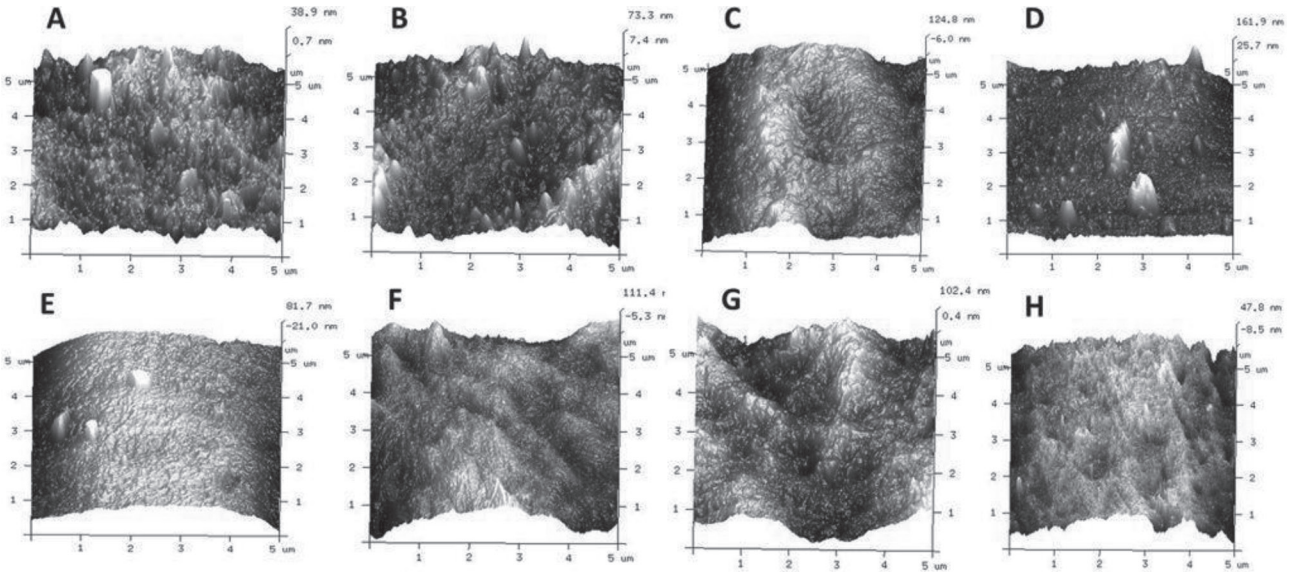

Figure 11. AFM images (height) (a) PU, (b) PU/SSMMP 7 h+SPR 3% 75:25, (c) PU/SSMMP 7 h+SPR 3% 25:75, (d) PU/SSMMP 24 h+SPR 3 % 75:25, (e) PU/SSMMP 24 h+SPR 3% 25:75, (f) PU/SSMMP 7 h 3%, (g) PU/SSMMP 24 h 3% and (h) PU/SPR 3%

influence the interactions between its layers and polyurethane chains[32].

4. CONCLUSIONS

Ternary nanocomposites were prepared by in situ polymerisation utilising SSMMPs and SPR clay as fillers, proving that it is possible to blend these fillers together. Structural analyses (XRD and FTIR) allied to morphological tests (TEM, SEM and AFM) demonstrated that the fillers are well dispersed/exfoliated into the polymeric matrix leading to nanocomposites PU/SSMMP/SPR with superior thermal and mechanical properties. Using blended fillers into a polyurethane

Table 2. Average roughness (Ra); root mean square roughness (Rq); maximum height roughness (Rmax) for the hybrid nanocomposites

Samples	Ra (nm)	Rq (nm)	Rmax (nm)
PU Pure	7.95	11	136
PU/SSMMP 7 h+SPR 3% 75:25	13.7	18	138
PU/SSMMP 7 h+SPR 3% 25:75	32.9	41.3	236
PU/SSMMP 24 h+SPR 3% 75:25	20.2	29.1	290
PU/SSMMP 24 h+SPR 3% 25:75	28.8	35	244
PU/SSMMP 7 h 3%	24.4	31.7	244
PU/SSMMP 24 h 3%	24.9	31.3	199
PU/SPR 3%	16.4	13.2	144

matrix results in materials that can perform functions that require high thermal and mechanical performance. These results corroborate previous studies showing that synthetic talcs are interesting to the development of materials with distinguished properties, and may also be combined with other fillers.

ACKNOWLEDGEMENTS

The authors would like to thank CAPES and CNPq for doctorate, post-doc and research scholarship. Also to Nokxeller – Microdispersions for providing SPR clay.

REFERENCES

1. X. Zhang, R. Xu, Z. Wu, C. Zhou, The synthesis and characterization of polyurethane/clay nanocomposites *Polymer International*, **52** (2003), 790–794.
2. B. Finnigan, D. Martin, P. Halley, R. Truss, K. Campbell, Morphology and properties of thermoplastic polyurethane nanocomposites incorporating hydrophilic layered silicates, *Polymer*, **45** (2004), 2249–2260.
3. N. Salahuddin, S.A. Abo-El-Enein, A. Selim, O.S. El-Dien, Synthesis and characterization of polyurethane/organo-montmorillonite nanocomposites, *Applied Clay Science*, **47** (2010), 242–248.
4. A.K. Barick, D.K. Tripathy, Effect of organically modified layered silicate nanoclay on the dynamic viscoelastic properties of thermoplastic polyurethane nanocomposites, *Applied Clay Science*, **52** (2011), 312–321.
5. G. Zhao, T. Wang, Q. Wang, Studies on wettability, mechanical and tribological properties of the polyurethane composites filled with talc, *Applied Surface Science*, **258** (2012), 3557–3564.
6. A. Dumas, F. Martin, C. Le Roux, P. Micoud, S. Petit, E. Ferrage, J. Brendlé, O. Grauby, M. Greenhill-Hooper, Phyllosilicates synthesis: a way of accessing edges contributions in NMR and FTIR spectroscopies. Example of synthetic talc, *Physics and Chemistry of Minerals*, **40** (2013), 361–373.
7. C. Saha, T.K. Chaki, N.K. Singha, Synthesis and characterization of elastomeric polyurethane and PU/clay nanocomposites based on an aliphatic diisocyanate, *Journal of Applied Polymer Science*, **130** (2013), 3328–3334.
8. M. Strankowski, J. Strankowska, M. Gazda, Ł. Piszczyk, G. Nowaczyk, S. Jurga, Thermoplastic polyurethane/(organically modified montmorillonite) nanocomposites produced by in situ polymerization, *Express Polymer Letters*, **6** (2012).
9. T.Y. Tsai, M.J. Lin, Y.C. Chuang, P.C. Chou, Effects of modified clay on the morphology and thermal stability of PMMA/clay nanocomposites, *Materials Chemistry And Physics*, **138** (2013), 230–237.
10. S. Anandhan, H.S. Lee, Influence of organically modified clay mineral on domain structure and properties of segmented thermoplastic polyurethane elastomer, *Journal of Elastomers & Plastics*, **46** (2014), 217–232.
11. S. Livi, J. Duchet-Rumeau, T.N. Pham, J.F. Gérard, Synthesis and physical properties of new surfactants based on ionic liquids: improvement of thermal stability and mechanical behaviour of high density polyethylene nanocomposites, *Journal of Colloid and Interface Science*, **354** (2011), 555–562.
12. F. Martin, P. Micoud, L. Delmotte, C. Marichal, R. Le Dred, P. De Parseval, A. Mari, J.P. Fortune, S. Salvi, D. Beziat, O. Grauby, J. Ferret, The structural formula of talc from the Trimouns deposit, Pyrénées, France, *The Canadian Mineralogist*, **37** (1999), 997–1006.
13. F. Martin, *International Patent*, 081046 (2009).
14. M. Yousfi, S. Livi, A. Dumas, C. Le Roux, J. Crépin-Leblond, M. Greenhill-Hooper, J. Duchet-Rumeau, Use of new synthetic talc as reinforcing nanofillers for polypropylene and polyamide 6 systems: thermal and mechanical properties, *Journal of Colloid and Interface Science*, **403** (2013), 29–42.
15. A. Dumas, F. Martin, E. Ferrage, P. Micoud, C. Le Roux, S. Petit, Synthetic talc advances: Coming closer to nature, added value, and industrial requirements, *Applied Clay Science*, **85** (2013), 8–18.
16. M. Song, D.J. Hourston, K.J. Yao, J.K. Tay, M.A. Ansarifar, High performance nanocomposites of polyurethane elastomer and organically modified layered silicate, *Journal of Applied Polymer Science*, **90** (2003), 3239–3243.
17. H. Jin, J.J. Wie, S.C. Kim, Effect of organoclays on the properties of polyurethane/clay nanocomposite

coatings, *Journal of Applied Polymer Science*, **117** (2010), 2090–2100.

18. A.F. Osman, K. Jack, G. Edwards, D. Martin, Effect of processing route on the morphology of thermoplastic polyurethane (TPU) nanocomposites incorporating organofluoromica, *In Advanced Materials Research*, **832** (2014), 27–32.
19. S. Taheri, G.M. Sadeghi, Microstructure–property relationships of organo-montmorillonite/polyurethane nanocomposites: Influence of hard segment content, *Applied Clay Science*, **114** (2015), 430–439.
20. V.D. da Silva, L.M. dos Santos, S.M. Subda, R. Ligabue, M. Seferin, C.L. Carone, S. Einloft, Synthesis and characterization of polyurethane/titanium dioxide nanocomposites obtained by in situ polymerization, *Polymer Bulletin*, **70** (2013), 1819–1833.
21. M.A. Prado, G. Dias, C. Carone, R. Ligabue, A. Dumas, C. Le Roux, P. Micoud, F. Martin, S. Einloft, Synthetic Ni-talc as filler for producing polyurethane nanocomposites, *Journal of Applied Polymer Science*, **132** (2015).
22. G. Dias, M.A. Prado, C. Carone, R. Ligabue, A. Dumas, F. Martin, C. Le Roux, P. Micoud, S. Einloft, Synthetic silico-metallic mineral particles (SSMMP) as nanofillers: comparing the effect of different hydrothermal treatments on the PU/SSMMP nanocomposites properties, Polymer *Bulletin*, **72** (2015), 2991–3006.
23. G. Dias, M. Prado, C. Carone, R. Ligabue, A. Dumas, C. Le Roux, P. Micoud, F. Martin, S. Einloft, Comparing different synthetic talc as fillers for polyurethane nanocomposites, *Macromolecular Symposia*, **367** (2016), 136–142.
24. L. M. dos Santos, R. Ligabue, A. Dumas, C. Le Roux, P. Micoud, J. F. Meunier, F. Martin, S. Einloft, New magnetic nanocomposites: Polyurethane/Fe_3O_4-synthetic talc, *European Polymer Journal*, **69** (2015), 38–49.
25. L.M. dos Santos, R. Ligabue, A. Dumas, C. Le Roux, P. Micoud, J. F. Meunier, F. Martin, M. Corvo, P. Almeioda, S. Einloft, Waterborne polyurethane/Fe_3O_4-synthetic talc composites: synthesis, characterization and magnetic properties, *Polymer Bulletin*, (2017), 1–16.
26. A. Dorigato, A. Pegoretti, A. Penati, Effect of the polymer-filler interaction on the thermo-mechanical response of polyurethane-clay nanocomposites from blocked prepolymer, *Journal of Reinforced Plastics and Composites*, **30** (2011), 325–335.
27. G. Verma, A. Kaushik, A.K. Ghosh, Preparation, characterization and properties of organoclay reinforced polyurethane nanocomposite coatings, *Journal of Plastic Film & Sheeting*, **29** (2013), 56–77.
28. M. Haghayegh, G. Mir Mohamad Sadeghi, Synthesis of shape memory polyurethane/clay nanocomposites and analysis of shape memory, thermal, and mechanical properties, *Polymer Composites*, **33** (2012), 843–849.
29. A. Kaushik, D. Ahuja, V. Salwani, Synthesis and characterization of organically modified clay/castor oil based chain extended polyurethane nanocomposites, *Composites Part A: Applied Science and Manufacturing*, **42** (2011), 1534–1541.
30. S.C. Amico, C.P. Freitag, I.C. Riegel, S.H. Pezzin, Efeito da incorporação de talco nas características térmicas, mecânicas e dinâmico-mecânicas de poliuretanos termoplásticos, *Revista Matéria*, **16** (2011), 597–605.
31. P.K. Maji, A.K. Bhowmick, Efficacy of clay content and microstructure of curing agents on the structure–property relationship of new-generation polyurethane nanocomposites, *Polymers for Advanced Technologies*, **23** (2012), 1311–1320.
32. G. Verma, A. Kaushik, A.K. Ghosh, Comparative assessment of nano-morphology and properties of spray coated clear polyurethane coatings reinforced with different organoclays, *Progress in Organic Coatings*, **76** (2013), 1046–1056.
33. S. Ramesh, K. Punithamurthy, The effect of organoclay on thermal and mechanical behaviours of thermoplastic polyurethane nanocomposites, *Digest Journal Of Nanomaterials And Biostructures*, **12** (2017), 331–338.
34. K. Malkappa, B.N. Rao, T. Jana, Functionalized polybutadiene diol based hydrophobic, water dispersible polyurethane nanocomposites: Role of organo-clay structure, *Polymer*, **99** (2016), 404–416.
35. Y. Zhou, V. Rangari, H. Mahfuz, S. Jeelani, P.K. Mallick, Experimental study on thermal and mechanical behavior of polypropylene, talc/polypropylene and polypropylene/clay nanocomposites, *Materials Science and Engineering: A*, **402** (2005), 109–117.
36. E. G Bajsić, V. Rek, B. O. Pavić, The influence of talc content on the thermal and mechanical properties of thermoplastic polyurethane/polypropylene blends, *Journal of Elastomers & Plastics*, **45** (2013), 501–522.
37. J. Pavlićević, M. Špírková, O. Bera, M. Jovičić, K.M. Szécsényi, J. Budinski-Simendić, The influence of bentonite and montmorillonite addition on thermal decomposition of novel polyurethane/organoclay nanocomposites, *Macedonian Journal of Chemistry and Chemical Engineering*, **32** (2013), 319–330.
38. Z.W. Liu, H.C. Chou, S.H. Chen, C.T. Tsao, C.N. Chuang, L.C. Cheng, C.H. Yang, C.K. Wang, K.H. Hsieh, Mechanical and thermal properties of thermoplastic polyurethane-toughened polylactide-based nanocomposites, *Polymer Composites*, **35** (2014), 1744–1757.

39. Y. Qin, J. Yang, M. Yuan, J. Xue, J. Chao, Y. Wu, M. Yuan, Mechanical, barrier, and thermal properties of poly(lactic acid)/poly (trimethylene carbonate)/talc composite films, *Journal of Applied Polymer Science*, **131** (2014).

40. M. Yousfi, S. Livi, A. Dumas, J. Crépin-Leblond, M. Greenhill-Hooper, J. Duchet-Rumeau, Compatibilization of polypropylene/polyamide 6 blends using new synthetic nanosized talc fillers: Morphology, thermal, and mechanical properties, *Journal of Applied Polymer Science*, **131** (2014).

41. H. Baniasadi, S. J S. A.A.R. Nikkhah, Investigation of in situ prepared polypropylene/clay nanocomposites properties and comparing to melt blending method, *Materials & Design*, **31** (2010), 76–84.

42. K. Wang, N. Bahlouli, F. Addiego, S. Ahzi, Y. Rémond, D. Ruch, R. Muller, Effect of talc content on the degradation of re-extruded polypropylene/talc composites, *Polymer Degradation and Stability*, **98** (2013), 1275–1286.

43. L.A. Castillo, S.E. Barbosa, N.J. Capiati, Influence of talc morphology on the mechanical properties of talc filled polypropylene, *Journal of Polymer Research*, **20** (2013), 152.

44. G.P. Balamurugan, S.N. Maiti, Effects of nanotalc inclusion on mechanical, microstructural, melt shear rheological, and crystallization behavior of polyamide 6-based binary and ternary nanocomposites, *Polymer Engineering & Science*, **50** (2010), 1978–1993.

45. A.K. Mohapatra, S. Mohanty, S.K. Nayak, Dynamic mechanical and thermal properties of polylactide-layered silicate nanocomposites, *Journal of Thermoplastic Composite Materials*, **27** (2014), 669–716.

46. T.F. Cipriano, A.L. Silva, A.H. Silva, A.M. Sousa, G.M. Silva, M.G. Rocha, Thermal, rheological and morphological properties of poly (lactic acid) (PLA) and talc composites, *Polímeros*, **24** (2014), 276–282.

47. A. Arora, V. Choudhary, D.K. Sharma, Effect of clay content and clay/surfactant on the mechanical, thermal and barrier properties of polystyrene/organoclay nanocomposites, *Journal of Polymer Research*, **18** (2011), 843–857.

48. H.M. Hassanabadi, D. Rodriguez, Effect of particle size and shape on the reinforcing efficiency of nanoparticles in polymer nanocomposites, *Macromolecular Materials and Engineering*, **299** (2014), 1220–1231.

49. S.M. Alavi, M. Esfandeh, J. Morshedian, Y. Jahani, Study of the Mechanical and Dynamic Mechanical Properties of Polypropylene/Talc/Nanoclay Ternary Nanocomposites, *Polymers & Polymer Composites*, **20** (2012), 299.

50. H. Aguilar, M. Yazdani-Pedram, P. Toro, R. Quijada, M. López-Manchado, Synergic effect of two inorganic fillers on the mechanical and thermal properties of hybrid polypropylene composites, *Journal of the Chilean Chemical Society*, **59** (2014), 2468–2473.

51. M. Kodal, S. Erturk, S. Sanli, G. Ozkoc, Properties of talc/wollastonite/polyamide 6 hybrid composites, *Polymer Composites*, **36** (2015), 739–746.

52. H. Garmabi, S.E.A. Tabari, A. Javadi, H. Behrouzi, G. Hosseini, An investigation on morphology and mechanical properties of HDPE/nanoclay/nano $CaCO_3$ ternary nanocomposites, *AIP Conference Proceedings*, **1713** (2016), 090005.

53. A. Dumas, C. Le Roux, F. Martin, P. Micoud, Process for preparing a composition comprising synthetic mineral particles and composition, WO2013004979 A1 (2013).

54. A.K. Mishra, S. Allauddin, R. Narayan, T.M. Aminabhavi, K.V. Raju, Characterization of surface-modified montmorillonite nanocomposites, *Ceramics International*, **38** (2012), 929–934.

55. J.D. Russell, V.C. Farmer, B. Velde, Replacement of OH by OD in layer silicates, and identification of the vibrations of these groups in infra-red spectra, *Mineralogical Magazine*, **37** (1970), 869–879.

56. M. Zhang, Q. Hui, X.J. Lou, S.A. Redfern, E.K. Salje, S.C. Tarantino, Dehydroxylation, proton migration, and structural changes in heated talc: An infrared spectroscopic study, *American Mineralogist*, **91** (2006), 816–825.

57. H. Chen, M. Wang, Y. Lin, C.M. Chan, J. Wu, Morphology and mechanical property of binary and ternary polypropylene nanocomposites with nanoclay and $CaCO_3$ particles, *Journal of Applied Polymer Science*, **106** (2007), 3409–3416.